Soil & Tillage Research 221 (2022) 105398

Contents lists available at ScienceDirect

Soil & Tillage Research

journal homepage: www.elsevier.com/locate/still

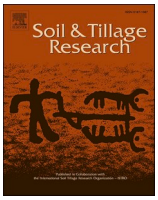

Maize root-induced biopores do not influence root growth of subsequently grown maize plants in well aerated, fertilized and repacked soil columns

Maxime Phalempin [a,*,1], Magdalena Landl [b,2], Gi-Mick Wu [c,3], Andrea Schnepf [b,4], Doris Vetterlein [a,d,5], Steffen Schlüter [a,6]

[a] Department of Soil System Sciences, Helmholtz-Centre for Environmental Research – UFZ, Halle (Saale), Germany
[b] Forschungszentrum Jülich GmbH, Agrosphere (IBG-3), Jülich, Germany
[c] Helmholtz Centre for Environmental Research – UFZ, PACE, Permoserstraße 15, 04318 Leipzig, Germany
[d] Soil Science, Martin-Luther-University Halle-Wittenberg, Germany

ARTICLE INFO

Keywords:
Biopore recycling
X-ray CT
Bulk density
Root growth modelling
Root decomposition
CPlantBox

ABSTRACT

Biopore recycling is the process during which roots ingress into existing biopores instead of creating new ones. Previous studies investigated biopore recycling in rather artificial conditions, e.g., with artificially created vertical macropores, by neglecting the smaller biopore diameter classes or by focusing on high bulk density soil material only. To address these shortcomings, we designed a soil column experiment and characterized the degree of biopore recycling for two soil textures (sand, loam) and two bulk density treatments (loam: 1.26 vs 1.36 g cm^{-3}, sand: 1.50 vs 1.60 g cm^{-3}). We developed a novel method based on the analysis of X-ray CT 3D images which enabled us to characterize the degree of biopore recycling for root-induced biopores down to 60 μm of diameter. The degree of biopore recycling was two orders of magnitude lower than previously reported in the literature (on average 0.0036 centimeters of roots were found in 1 centimeter of biopores). Roots were crossing the biopores rather than colonizing them. Visual analysis of the images showed that the propensity of roots to grow into biopores was higher when the angle at which roots and biopores touched was inferior to 45 degrees and when the root diameter was approximately equal to or inferior to the biopore diameter. There were no statistical differences for the biopore recycling fraction between the two bulk density treatments in loam. In loam, roots degraded quickly (less than 78 days) and the biopores created were stable over time. In sand, some biopores were still filled with root residues after 216 days and many biopores had collapsed. We conclude that biopore recycling is less likely to occur in sand, as compared to in loam. We further used the model CPlantBox to simulate root system architectures with identical root length density as observed in the experiment but random arrangement with respect to biopores. By comparing the modeling results with the experimental results, we showed that roots had no preference for growing into biopores under the studied conditions.

1. Introduction

Biopores are voids in soil resulting from the activity of living organisms. In agroecosystems, biopores play a key role for matter fluxes as well as for plant growth (Kautz, 2015). Biopores provide growing roots with a path of reduced mechanical impedance and therefore ease

Abbreviations: BD, Bulk Density; BLD, Biopore Length Density; BRF, Biopore recycling Fraction; CT, Computed Tomography; L, Loam; NCP, Normalized Number of Contact Points; RLD, Root Length Density; ROI, Region Of Interest; S, Sand.

* Correspondence to: Theodor-Lieser Straße 4., 06110 Halle (Saale), Germany.
E-mail addresses: maxime.phalempin@ufz.de (M. Phalempin), m.landl@fz-juelich.de (M. Landl), mick.wu@ufz.de (G.-M. Wu), a.schnepf@fz-juelich.de (A. Schnepf), doris.vetterlein@ufz.de (D. Vetterlein), steffen.schlueter@ufz.de (S. Schlüter).
[1] **ORCID ID:** 0000-0003-1198-807X
[2] **ORCID ID:** 0000-0002-8567-0454
[3] **ORCID ID:** 0000-0002-4093-0400
[4] **ORCID ID:** 0000-0002-7719-7476
[5] **ORCID ID:** 0000-0003-2020-3262
[6] **ORCID ID:** 0000-0002-3140-9058

https://doi.org/10.1016/j.still.2022.105398
Received 21 October 2021; Received in revised form 4 April 2022; Accepted 9 April 2022
Available online 20 April 2022
0167-1987/© 2022 The Author(s). Published by Elsevier B.V. This is an open access article under the CC BY-NC-ND license (http://creativecommons.org/licenses/by-nc-nd/4.0/).

the exploration of the available soil volume (Bengough and Mullins, 1990; Passioura, 2002), especially of deeper soil layers which are usually more compact. By allowing roots to reach deeper layers of the soil horizon, biopores also play an important role for the sequestration of carbon in the form of root necromass into the subsoil (Jones et al., 2009). During rainfall events, biopores influence the water budget by allowing a fast macropore flow of water (Dohnal et al., 2009), which in turn contributes to reducing water run-off and soil erosion (Ehlers, 1975; Kautz, 2015; Yunusa and Newton, 2003). Biopores also improve soil aeration in compacted soil (Colombi et al., 2017).

For a long time, the investigation of the nature and spatial distribution of biopores has been hampered by the opaque and fragile nature of the soil. Although biopores were observed and described as early as in the late 19th century (Hensen, 1892), the methods which would allow a rigorous measurement of the abundance and physical properties of biopores only came about approximately a century later. Such methods include the use of a soil peel method (Smettem and Collis-George, 1985), profile wall method (Han et al., 2015), horizontal minirhizotrons (Wahlström et al., 2021), rhizotrons (Bauke et al., 2017), in situ endoscopy (Athmann et al., 2014, 2013; Kautz and Köpke, 2010; Pagenkemper et al., 2015), isotope labelling (Banfield et al., 2017), photography (Nakamoto, 2000) and X-ray computed tomography (CT) (Atkinson et al., 2020; Cheik et al., 2021; Colombi et al., 2017; Lucas et al., 2021; Pagenkemper et al., 2015; Pfeifer et al., 2014; Zhang et al., 2018; Zhou et al., 2021). The development of those methods paved new ways for the study of the ecological relevance of biopores.

The term "biopore recycling" or "biopore reuse" refers to the process during which roots ingress into existing biopores instead of creating new ones. In agroecosystems, biopore recycling is usually considered to occur in the subsoil as it is the zone where biopores can pertain for decades (Hagedorn and Bundt, 2002). In the topsoil, the presence of biopores is rather short-lived because the soil structure is more dynamic and is usually subjected to tillage.

The degree of biopore recycling is typically gauged by comparing the actual occurrence of roots in biopores to some random configuration as a control. In doing so, Dexter (1986) found that there was no evidence for the roots sensing and growing preferentially towards artificially created biopores in a well-aerated system, supporting the argument of indifference of roots towards biopores. Nakamoto (1997) came to similar conclusions after comparing the calculated probability of roots entering biopores and the experimentally measured proportion of roots in artificial macropores.

Supporting the argument of preference of roots towards biopores, Stewart et al. (1999) showed that approximately 5–15% more roots were found in and around pre-existing macropores than expected at random, in two black coarsely structured vertisols. With densely packed soil columns (1.78 g cm^{-3}) and artificially created vertical macropores (3.2 mm of diameter), Stirzaker et al. (1996) showed that the number of roots found in macropores was much higher as compared to the calculated probability that a root enters a biopore. In a rhizotron study with a silty loam subsoil compacted at 1.40 g cm^{-3}, Bauke et al. (2017) observed that more roots grew into macropores than if root growth in macropores was driven only by chance. The preference of roots to grow towards biopores in compacted soil was also demonstrated with X-ray CT studies and its benefit for plant growth was confirmed (Colombi et al., 2017; Pfeifer et al., 2014).

Using artificially created vertical pores, Nakamoto (1997) found that the degree of biopore reuse for *Zea mays L.* c.v Nagano´ranged from 14% at 15 cm depth up to 33% at 40 cm depth. Similar values of biopore recycling were also reported by Athmann et al. (2013) and Han et al. (2017). Biopore reuse rates can be further distinguished into colonization, i.e. when roots enter the macropore and elongate in it, and crossing, i.e. when roots directly leave the macropore again. The degree of colonization was only 14% for barley roots in a compacted soil (bulk density 1.64 g cm^{-3}, mechanical resistance: 1.4 MPa) (Pfeifer et al., 2014). This percentage of colonization on all interaction events differed substantially for wheat roots between a loose soil (1.2 g cm^{-3}, 1.1 MPa) and a compacted soil (1.57 g cm^{-3}, 2.9 MPa) and amounted to 13% and 69%, respectively (Atkinson et al., 2020). In pot experiments (1.60 g cm^{-3}, 1.0 MPa) with different plants this fraction differed between maize (62%), soybean (48%) and wheat (20%), likely due to different tolerance to increased mechanical impedance or different root-soil contact caused by different root diameters (Colombi et al., 2017). In contrast, wheat roots were more frequently found in biopores than maize roots (<1 MPa) (Nakamoto, 2000), which was explained by the fact that the thinner root tips of wheat were able to change their direction more easily and colonize biopores.

In the literature, it is still debated controversially how roots are able to "sense" the presence of biopores and grow towards them; a mechanism coined trematropism by Dexter (1986). It has been proposed that root growth in biopores is simply the result of roots preferentially elongating in zones of the soil where the mechanical impedance is lower (Stirzaker et al., 1996). Stirzaker et al. (1996) further hypothesized that roots might be able to detect biopores by growing towards the microcracks that are formed ahead of the root tip and that these microcracks may lead to other structurally weak zones such as a biopore. In pot experiments with artificial macropores, roots need to overcome compacted areas around the macropore before entering them. Therefore, oxytropism might be a better explanation as biopores also offer a rather continuous and higher supply of oxygen as compared to the bulk soil (Colombi et al., 2017; Gliński and Lipiec, 2018; Pfeifer et al., 2014), which is favorable for root growth (Crawford, 1992). Even though bulk density may increase around biopores the mechanical resistance in the vicinity of biopores is still reduced due to a reduction in radial confining pressure, rendering both mechanical impedance and oxygen supply as possible mechanisms to explain to observed attraction of roots (Atkinson et al., 2020). Moreover, roots may exhibit chemotropism towards biopores since the concentration of carbon, nitrogen, phosphorus and the microbial activity might be increased in the wall of macropores (Barej et al., 2014; Pankhurst et al., 2002; Vinther et al., 1999). This chemotropism might be induced by the presence of nitrate and glutamate sensors present at the root tip (Filleur et al., 2005). On the other hand, biopores may be associated with certain pathogens (Pankhurst et al., 2002; Rasse and Smucker, 1998), which may cause the roots to be rather indifferent to the biopores or avoid them instead of growing towards or into them.

Based on the literature, it seems that the extent to which the roots reuse biopores might be the result of interacting factors such as soil penetration resistance (Stirzaker et al., 1996), soil depth (Nakamoto, 1997), plants species (Nakamoto, 2000; Rasse and Smucker, 1998), biopore geometry, abundance and relief (Hirth et al., 2005) and biopore origin (Athmann et al., 2014; Kautz et al., 2014). Our review of the literature revealed some shortcomings of existing studies on biopore recycling. Indeed, some studies investigated the behavior of roots in vertical artificially created macropores (i.e., macropores created by pushing a rod or a wire into the soil) (Atkinson et al., 2020; Bauke et al., 2017; Colombi et al., 2017; Dresemann et al., 2018; Hirth et al., 2005; Nakamoto, 1997; Pfeifer et al., 2014; Stirzaker et al., 1996). Considering the properties of biopores and, in light of the response of roots to their growing environment, root growth in artificially created macropores is likely somewhat unrealistic and not representative of root growth in pores created by living organisms. Other studies used experimental methods and measuring devices which limit the size range of the biopores investigated, e.g., the use of a 3.8 mm in diameter endoscope (Athmann et al., 2013) or X-ray CT analysis with a voxel resolution that is too coarse to detect fine roots (Colombi et al., 2017; Zhou et al., 2021). Such methods inherently introduce a bias towards the investigation of the largest diameter class of biopores (in the range of millimeters in diameter for endoscopy) and might have drawn conclusions disregarding the behavior of roots in the smallest diameter class of biopores (in the range of micrometers in diameter). Finally, other studies focused exclusively on subsoil material (Bauke et al., 2017; Han et al., 2017;

Nakamoto, 2000; Wahlström et al., 2021; White and Kirkegaard, 2010), in which biopore stability is likely increased due to an increased mechanical impendance of the subsoil by overburden pressure and the presence of $CaCO_3$ as a cementing agent.

In order to address these shortcomings, we designed a soil column experiment and characterized the degree of biopore reuse occurring in repacked soil columns under controlled conditions. We developed a novel method based on the analysis of X-ray CT derived 3D images which enabled us to characterize the degree of biopore reuse for root-induced biopores down to 60 μm of diameter. The method is based on the repeated scanning of soil samples and co-registration of the acquired images after the creation of biopores and their potential reuse. With this method, we investigated the following hypotheses:

1. The reuse of biopores is influenced by soil texture. It is expected to observe different behavior of biopores as a result of different cohesive forces met by the soil particles of varying sizes. We expect that biopores in a coarse textured soil will be more prone to collapsing and that this will affect the degree of biopore recycling. This hypothesis was investigated by analyzing the degree of biopore recycling for a fine textured (i.e., loam) and a coarse textured soil (i.e., sand).
2. Keeping all other factors constant, the reuse of biopores is higher in a substrate with higher penetration resistance. Since under constant soil moisture soil penetration resistance is proportionally correlated to the bulk density of a porous medium (Hernanz et al., 2000), it is expected that the degree of biopore recycling will increase concomitantly with bulk density. This hypothesis was investigated by introducing a factor "soil bulk density" in our analysis.

In addition to addressing these hypotheses, a new approach to study biopore recycling *in silico* was developed. The purely stochastic root growth model CPlantBox (Schnepf et al., 2018) was used to characterize the degree of biopore recycling which could be expected at random and the latter was compared with the experimental results. The newly developed X-ray CT based method and the associated modelling approach enabled us to shed light on the circumstances under which roots reuse biopores or not.

2. Material and methods

2.1. Soil and plant material

The substrate loam (L) was obtained from the upper 50 cm of a haplic Phaeozem soil profile in Schladebach, Germany (51°18′31.41′′ N; 12°6′16.31′′ E) that had been under agricultural use and last planted with oilseed rape before excavation. It was dried to 0.1 g g^{-1} gravimetric water content by evaporation and then sieved down to 1 mm. The substrate sand (S) constitutes a mix of 83% quartz sand (WF 33, Quarzwerke Weferlingen, Germany) and 17% of the sieved loam. Details on chemical and physical properties are provided elsewhere (Vetterlein et al., 2021). In loam the gravimetric contents of sand, silt, clay, soil organic carbon and total nitrogen were 33%, 48%, 19%, 0.84% and 0.084%, respectively. In sand they amounted to 89%, 8%, 3%, 0.14% and 0.014%. The *Zea mays* L. genotype B73 wild-type (WT) was selected for the growth experiments.

2.2. Experimental design and set-up

The experiment was designed in three phases. In the first phase, roots were allowed to grow freely in repacked soil columns. After the end of the growth experiment, subsamples (i.e., ingrowth cores) were taken. The ingrowth cores consisted of plastic cylinders perforated at the sidewall, the top and bottom with a 2 mm diameter drill so that roots could enter from all sides. In the second phase, the ingrowth cores were incubated and stored under conditions which would allow the roots inside the ingrowth cores to degrade. In the third phase, the ingrowth cores containing biopores were reburied inside newly packed soil columns. The soil columns of phase 3 were then planted and roots were allowed to grow in and around the ingrowth cores (containing biopores). The technical aspects associated with each phase of the experiment are described below. Fig. 1 gives an overview of the experimental design and set-up of the experiment.

2.2.1. Phase 1 – Root growth

Prior to packing the columns, the soil was fertilized in the same fashion as in Lippold et al. (2021). After fertilization, the columns (18 cm height, 10 cm inner diameter) were packed by gradually placing the soil in layers of 1.8 cm and gently consolidating each layer. The columns were packed to different bulk densities in order to investigate the effect of soil compaction on biopore recycling. For the low bulk density treatment, four columns per soil texture were packed to 1.26 and 1.50 g cm^{-3} for the loam and the sand, respectively. The X-ray CT derived particle size distribution capturing individual sand grains and fine-textured aggregates showed a peak at 100 μm and 200 μm for loam and sand, respectively (Fig. S1). For the high bulk density treatment, four columns per soil texture were packed to 1.36 and 1.60 g cm^{-3} for the loam and the sand, respectively. The growth experiment was conducted in a climate chamber (Vötsch Industrietechnik GmbH) that was set to 22 °C during the day and 18 °C at night with a 12-hour light-period, 350 μM m^{-2} s^{-1} of photosynthetically active radiation and a constant relative humidity at 65%.

Soil volumetric water content was tested in trial experiments in order to ensure appropriate soil moisture conditions for plant growth and to avoid water logging in the bottom part of the columns. The retained average volumetric water content values were 22% and 18% for loam and sand, respectively. At this volumetric water content, the penetration resistance for the low bulk density treatment for repacked samples is approximately equal to 0.15 MPa and 0.08 MPa for the loam and the sand, respectively (Fig S2; U. Rosskopf, S. Peth, D. Uteau, University Hannover, personal communication). Mechanical resistance data at the higher bulk density levels is not available for the repacked samples as used in this study. However, for undisturbed field samples with the same substrates and bulk densities varying between 1.3 and 1.5 g cm^{-3} for loam and 1.4 and 1.6 g cm^{-3} for sand, penetration resistance at a soil matric potential of − 3 kPa is in the range of 0.5–1.2 MPa for sand and loam (Rosskopf et al., 2022). Penetration test were performed at 120 mm h^{-1} using a universal testing machine with a high precision sensor equipped with a penetrometer conus resembling a root.

Before seeding the columns, maize seeds were surface sterilized for 5 min in 10% hydrogen peroxide and then left to soak for 3 h in a saturated calcium sulfate solution. One seed was placed at a depth of 1 cm in each soil column. The soil surface was covered with quartz gravel (3 – 6 mm in size) to reduce evaporation. Harvest was conducted on day 22 after planting. This growth duration corresponded to the BBCH14 plant growth stage (i.e., four leaves unfolded). At the end of the growing period, the plants were cut and left to dry in the oven at 65 °C for 3 days in order to determine shoot dry weight. Directly after cutting the shoot, six ingrowth cores per column (3 cm in diameter and height) were extracted with a subsampling device (UGT GmbH) at 5, 10 and 15 cm depth from the soil surface. The two ingrowth cores per soil depth were aligned along the central diameter and had the same spacing between them and the wall. This sampling procedure yielded a total of 96 ingrowth cores to analyze, which were stored at 4 °C in sealed plastic containers prior to X-ray CT scanning.

2.2.2. Phase 2 – Biopore creation

After X-ray CT scanning, the ingrowth cores were stored in an incubator set at a constant temperature of 25 °C. The ingrowth cores were kept in plastic bags along with a damp cloth so that moist conditions were maintained. Occasionally, the bags were opened and visually inspected to make sure that no mold was growing inside. The duration of

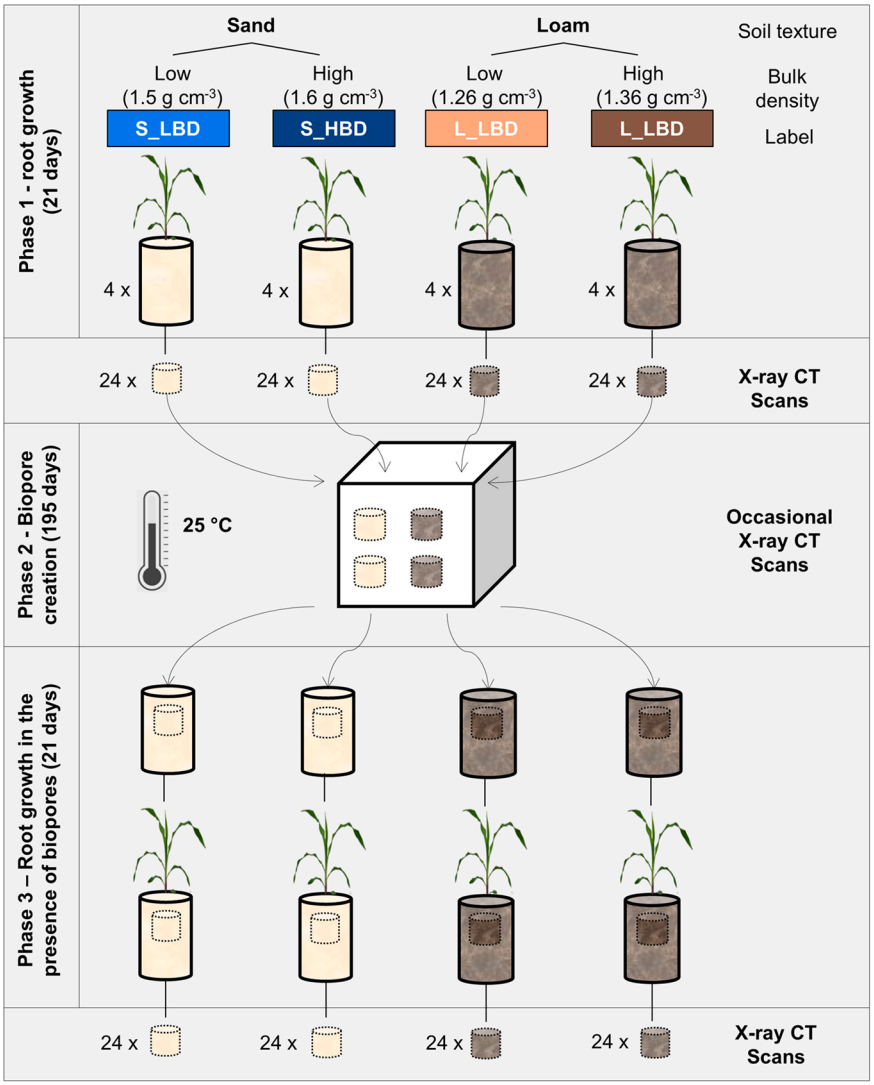

Fig. 1. Overview of the experimental design and set-up.

incubation was 195 days. At day 78 and 115, some cores were re-scanned with X-ray CT in order to assess the state of decomposition of the roots and the potential collapsing of biopores.

2.2.3. *Phase 3 – Root growth in the presence of biopores*

After phase 2, the ingrowth cores were buried again in newly packed soil columns at the same depths from which they were extracted. The plant growth conditions and experimental set-up were the same as for phase 1. However, the seeding procedure was modified. For phase 3, the seeds were pre-germinated in small containers (height: 4 cm, diameter: 2.5 cm) in order to make sure that every column would receive a fully germinated seed. Once the seeds were fully germinated, the small containers were reburied at the surface of the soil columns. After the growing period of 22 days, the ingrowth cores were extracted from the column and were stored at 4 °C in sealed plastic containers prior to X-ray CT scanning.

2.3. *X-ray computed tomography scanning*

X-ray CT scanning was performed with an industrial µCT scanner (X-TEK XTH 225, Nikon Metrology) having an Elmer-Perkin 1620 detector panel (1750 × 2000 pixels). The scanner was operated at 130 kV and 150 µA. A total of 2500 projections with an exposure time of 708 ms each were acquired during a full rotation of a sample. The obtained images were reconstructed into a 3D tomogram via a filtered back projection algorithm with the CT Pro 3D software (Nikon metrology). The resulting grayscale images had an 8-bit depth and a voxel size of 19 µm. The conversion to 8-bit allowed saving space without losing considerable information. During the 8-bit conversion, the grayscale range was normalized with a percentile stretching method. This method sets the darkest and brightest 0.2% voxels to 0 and 255, respectively, and performs a linear stretching in between.

2.4. *Root segmentation*

Root segmentation was performed with a modified version of the root segmentation algorithm "Rootine v.2″ (Phalempin et al., 2021a). Rootine v.2 is a free macro available for the free image analysis software Fiji/ImageJ (Schindelin et al., 2012). In addition to gray value information, Rootine v.2 is based on the shape detection of cylindrical roots. Some of the key steps of Rootine v.2 and modifications of the original version for this study (when applicable) are briefly described below.

After X-ray CT scanning, all images were visually analyzed and samples devoid of roots were not considered for analysis. For the remaining samples, circular region of interests (ROI) were defined. After defining the ROI, the images were subjected to preprocessing steps. First, the images were filtered with a 3D non local means filter (Tristán-Vega et al., 2012) available in the ITK library (McCormick et al.,

2014). After filtering, a step of edge enhancement was performed with the "Unsharp Mask" filter available in ImageJ. Then, a background removal step was applied via an "absolute difference transform" described by Phalempin et al. (2021a).

Rootine v.2 is tailored for the segmentation of roots in whole columns scans, where all roots enter the field of view through the top boundary and the image resolution is close to the smallest root diameter to segment. For whole columns scans, the distribution of root diameters is continuous within a range that is plant species-dependent. For the samples used in this study, the distribution of root diameters is not continuous but rather discrete, considering that roots of different types and orders can be present within a sample and vary substantially amongst all samples in a dataset. To cope with this discreteness, Rootine v.2 was modified in order to perform a "root diameter targeted approach" instead of using a "root diameter incremented approach", as implemented in the original version of Rootine v.2. With the new approach, every image was visually analyzed and the diameter of the roots in the image was measured using the "Measure" tool available in ImageJ. The sigma values of the tubeness filter implemented in ImageJ were then calculated based on the measured root diameters according to the formalizing steps described elsewhere (Phalempin et al., 2021a). The results of the tubeness filter were segmented using the "3D Hysteresis Thresholding" (Ollion et al., 2013) available in ImageJ.

After root segmentation, the obtained images were subjected to post-processing steps. First, a 3D median filter available in ImageJ was applied in order to smoothen the root surface. In the original version of Rootine v.2, small isolated objects are discarded by using a connectivity criterion of the root branches from top to bottom, which is tailor-made for whole column scans. For the samples as used in this study, roots can enter the ROI from all sides. In order to cope with this, Rootine v.2 was modified and the connectivity criterion was replaced by a size exclusion criterion in order to get rid of every object whose size fell under a user-defined threshold. The size exclusion step was performed with the "Size Opening (2D/3D)" plugin available in the "MorphoLibJ" plugin suite (Legland et al., 2016). The size exclusion threshold was set to 4000 voxels.

With the obtained images, several properties of the roots within the ingrowth cores were computed. The root length was calculated after a step of skeletonization with the "Skeletonize (2D/3D)" plugin available in the BoneJ plugin (Doube et al., 2010). The root diameter was computed with the "Local Thickness" plugin available in ImageJ. This plugin relies on the "Maximum Inscribing Sphere" method and assigns to every root voxel a value corresponding to the diameter of the largest sphere which locally fits into the root.

2.5. Image registration

The images obtained after phase 1 and phase 3 had different orientation with respect to the source of X-rays in the scanner. In order to cope with this, image registration was necessary to align the images. Non-rigid image registration was carried out with the software Elastix (Klein et al., 2010; Shamonin et al., 2014). Finding landmarks (i.e. points defined on the same locations in the two 3D volumes to register) was facilitated by the use of the plugin "Big Warp" available in ImageJ. Landmarks were set on easily identifiable objects like grains with impurities or pointy edges and were widely spread across the entire volume. The number of landmark pairs per image was adapted to the quality of the registration and ranged from four to nine.

2.6. Modeling approach

The root architecture model CPlantBox (Schnepf et al., 2018) was used to simulate three-week-old root systems of *Zea mays* growing within the boundaries of the soil columns used in the experiment. As a baseline parameter set for the root architecture model, the maize root parameters reported in Landl et al. (2021) were used. The baseline parameter set was then optimized so that the average root length density (RLD) obtained with CPlantBox matched the experimentally measured RLD. The root parameters with the greatest impact on the RLD distribution were selected for the optimization. These parameters are the mean elongation rate of basal roots, the distribution of the number of basal roots and the distribution of the inter-branch distances of basal roots and first order laterals. For the optimization procedure, the Broyden–Fletcher–Goldfarb–Shanno algorithm (Fletcher, 2013), which is available in Python 3.8, was used. The evaluation of the match between the modelled RLD and experimental RLD was done for the three ingrowth cores that were taken at depths 5, 10 and 15 cm. The optimization of the root growth parameters was done for phase 1 and for phase 3, respectively. After the optimization of the root growth parameters, 20 root system realizations were calculated for each phase. In analogy with the experimental dataset, these 40 root system realizations constitute two datasets of 20 modelled soil columns, i.e. one dataset for the phase 1 of the experiment and one dataset for the phase 3 of the experiment.

In the root architecture model CPlantBox, a root system is represented as connected line segments, in the form of vector data. In order to compare the results of CPlantBox with the experimental results, it was necessary to convert this representation of the root systems into a raster representation. The Bresenham's line algorithm was used to determine the voxels of a 3D grid needed to form a good approximation of a straight line between two root nodes. This resulted in root systems represented by single-voxel lines. The resolution of the 3D raster grid was set to 60 μm, which was the minimum observed root diameter.

Similarly to the optimization of the RLD, the diameter distribution in the simulated ingrowth cores was optimized so that the difference between the measured and simulated mean diameters was minimal. Note that the maximum allowed diameter was constrained to 900 μm in order to reduce the dilation step to a reasonable amount of time. After the optimization of the root diameter, each root voxel was dilated with a 3D ball-shaped kernel using the multiprocessing package available in Python. This resulted in a 3D rasterized representation of the root systems, in which each root segment was represented by a cylinder of a given diameter.

In the modelling approach, the characterization of biopore recycling within the modelled soil cores was evaluated by considering all possible combinations between the 20 modelled root system realizations of each phase. However, the possible combinations between the three different soil depths were not considered. Practically, this means that a simulated ingrowth core located at 5 cm depth in the simulated root system number 1 of phase 1 was compared with the simulated ingrowth cores located at 5 cm depth of the simulated root systems 1, 2, 3, and so forth up to the 20th simulated root system of phase 3. This yielded a total number of 400 combinations between the cores of phase 1 and the cores of phase 3 for each depth, i.e. 1200 combinations for the whole modelling dataset.

2.7. Data analysis and model comparison

Two metrics were used as a proxy for biopore recycling, namely the biopore recycling fraction (BRF) and the normalized number of contact points (NCP). The BRF was characterized by computing the root length found in a given biopore length. The BRF is expressed in a fraction of number of voxels [-] and is therefore dimensionless. The NCP was characterized by counting the occurrence of a root touching a biopore, normalized by the volume of the sample. It is therefore expressed in [1 cm^{-3}].

In order to calculate the NCP, the root systems of both phases were combined into one image, making sure that one gray value was assigned to the roots grown during phase 3, one gray value was assigned to biopores and another gray value was assigned to the combination of roots grown during phase 3 and the biopores. With a single thresholding method, the combined images were segmented in order to isolate the

voxels where roots and biopores touched. Then, the number of contact points was calculated with the "Connected Component Labelling" operation available in the MorphoLibJ plugin library (Legland et al., 2016). Note that, for the experiment dataset, all contact points having a size inferior to ten voxels were considered as artefacts and were therefore excluded from the analysis. Artefacts were occasionally created when a root and a biopore were slightly over-segmented and/or not perfectly registered. In that case, it was sometimes observed that some small artificial contact points were created. This phenomenon was mostly observed when a root and biopore touching one another were almost parallel. For the simulated dataset, all contact points were considered since there were no artefacts introduced by root over-segmentation or imperfect registration.

In this work, we hypothesize that the difference between the NCP obtained experimentally (NCP_{exp}) and the NCP obtained with CPlantBox (NCP_{mod}) is a valid metric to characterize the tendency of roots to grow towards, avoid or be indifferent to biopores. To generate the NCP_{mod} dataset, we used the formulation of CPlantBox which does not account for any preferential growth of roots towards, into or away from biopores. With this formulation, the model can be used as a benchmark to determine the number of times that roots and biopores touch at random. Considering this, we assume the following:

$$NCP_{exp} - NCP_{mod} \quad < 0;\ \textit{roots avoid biopores}$$

$$NCP_{exp} - NCP_{mod} \quad \approx 0;\ \textit{roots are indifferent to biopores}$$

$$NCP_{exp} - NCP_{mod} \quad > 0;\ \textit{roots grow towards biopores}$$

Of course, the likelihood that roots touch biopores at random is positively correlated to the amount of roots and biopores present. To take this into account, we modelled NCP as a function of biopore length density (BLD) (i.e., the RLD observed during phase 1) and the RLD in phase 3 using tensor product smooths to fit a 2D response surface in the framework of Generalized Additive Models (Wood, 2017). We modelled the raw counts of contact points (prior to normalization) using a negative binomial distribution and included an offset in the model to account for the volume of the soil samples. Treatment (simulated vs measured) was added to the model to estimate the difference between the number of contact points expected by the CPlantBox model and the experimental data. The generalized additive model enabled to predict the NCP_{exp} and the NCP_{mod} for all possible combinations of BLD and RLD interpolated between the observed values and constrained within the range of values observed.

2.8. Visual analysis of contact points

For some instances where roots and biopores touched, a visual analysis of the contact points was carried out in order to understand the circumstances under which roots were reusing biopores or not. A focus was made on the angle of contact between the roots and the biopores as well as the root and biopore diameter. In order to measure the contact angle, the two 2D planes that were spanned by the roots and the biopores at their intersection were found with the help of the plugin "Big Warp" available in ImageJ. Once the two 2D planes were found, the angle of contact was measured with the "Angle measurement tool" available in ImageJ. The evaluation of root and biopore diameter was only qualitative and was made visually.

2.9. Statistical analysis

Other statistical analyses were carried out to test whether the means of the different treatments significantly differed from one another (i.e., one-way ANOVA). Multiple pairwise-comparisons with Tukey HSD tests enabled to determine whether the mean difference between specific pairs of treatments were statistically significant. Unpaired Wilcoxon tests were performed when analyzing two independent groups having non-normally distributed data. All the data analysis was carried out in R Studio 3.5 using the multcomp (Hothorn et al., 2008), car (Fox et al., 2012), Tydiverse (Wickham et al., 2019), plyr (Wickham, 2020), mgcv (Wood, 2011) and ggplot2 (Wickham and Chang, 2016) libraries.

3. Results

3.1. Plant growth and root growth

The plant growth and root growth observed for the growth experiment of phase 1 and phase 3 differed substantially. This was reflected in the measurement of shoot dry weight (Fig. 2a), root length density (Fig. 2b) and the number of ingrowth cores containing roots (Fig. 2c). The shoot dry weight was approximately two times lower for phase 3 as compared to phase 1. This difference was even bigger for the root growth as root length density was an order of magnitude lower for phase 3 as compared to phase 1. Due to the different methods used for germination of the seeds, a time-lag of approximately 7 days of growth was observed in phase 3 as compared to phase 1. This is supported by the analysis of the evapotranspiration and the soil volumetric water content measured during the growth experiments (Fig. S3 and S4). Note that since this study focuses on roots exclusively, this difference of root growth has no consequences for the validity of biopore recycling results but only affects the range of RLD and BLD investigated. The effect of substrate and bulk density was weaker for the shoot dry weight as compared to the root length density. Despite the fact that differences were not statistically significant, the shoot dry weight and the root length density were systematically lower for the high bulk density treatment as compared to the low bulk density treatment and this was true for both loam and sand.

Since the analysis of BRF and NCP can only be performed when roots from the two growth experiments are present within a given ingrowth core, the number of samples containing roots for the combination of phase 1 and phase 3 was calculated (Fig. 2c). For loam, the number of samples containing roots was high and equal to 21 and 20 out of 24 for the low and high bulk density treatment, respectively. For sand, the number of samples containing roots was low and amounted to seven and two out of 24 for the low and high bulk density treatment, respectively. Differences in root growth in loam in comparison to sand have already been observed in a similar growth experiment (Lippold et al., 2021), however, the mechanisms behind this difference are still unknown.

3.2. Root degradation

The occasional X-ray CT scans performed at day 78 and 115 after the growth experiment of phase 1 provided insights into the time it took for roots to degrade and empty biopores to be formed. For loam, it took maximum 78 days for roots to decompose (Fig. 3a) and leave behind completely empty biopores. For sand, the root degradation was much slower as some roots were only partially shrunken after 115 days of incubation. After the end of the growth experiment of phase 3, i.e., after 216 days after the end of phase 1, some biopores in sand were still partially filled with old root tissues (Fig. 3b).

The occasional X-ray CT scans also enabled to acquire qualitative information regarding the stability of the biopores in loam and sand. For loam, the biopores were stable over time and the roots present after the first growth experiment could be very easily and precisely delineated when analyzing the biopores that they left behind after their decomposition (Fig. 3a). For sand, the arrangement of sand grains was rather fragile and movements of the sand grains in all possible directions (i.e. subsidence and lateral displacement) were frequently observed (Fig. 3b). When full decomposition of the roots was observed in sand, some biopores subsequently collapsed and/or were partially "refilled" with sand grains from their vicinity (Fig. 3c).

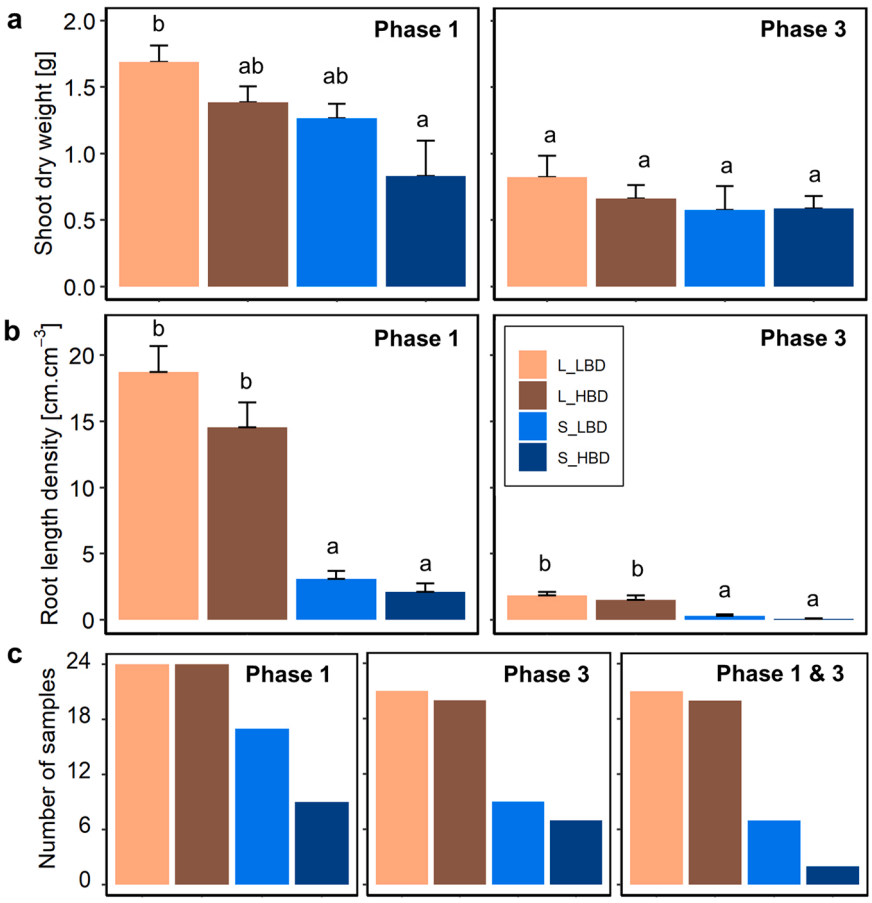

Fig. 2. Plant growth and root growth measured for the two growth experiments. (a) The shoot dry weight. (b) The root length density. (c) The number of samples containing roots in phase 1, phase 3 and the combination of phase 1 and 3. The error bars denote the standard error. The letters on top of the error bars denote pairwise-comparison between the mean of the treatments as assessed by a Tukey HSD test with $\alpha = 0.05$. The legend in subFig. b is also valid for subFigs. a and c.

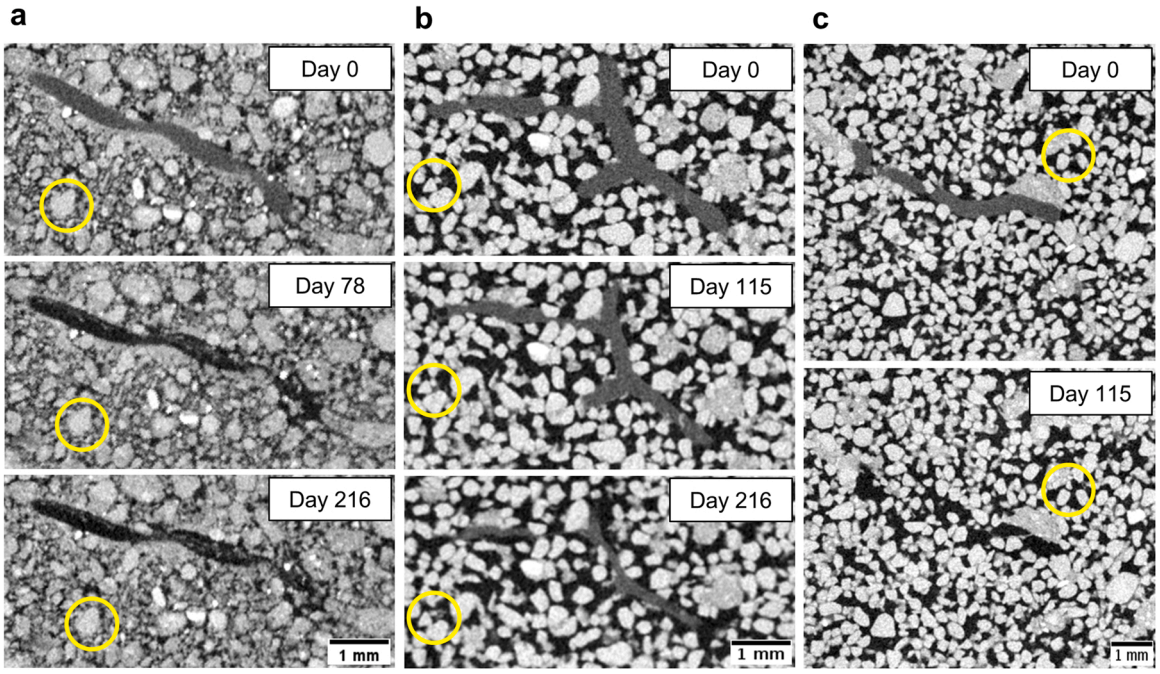

Fig. 3. Two dimensional X-ray CT images acquired at different times after the end of the growth experiment of phase 1. For better orientation, the yellow circles indicate grains which are common in the images. In loam, roots degraded quicker than in sand and left behind biopores which were structurally stable over time (subfigure a). In sand, old root tissues were sometimes observed even after 216 days of incubation time (subfigure b). When complete root degradation was observed in sand, the biopores were often refilled with sand grains from their vicinity (subfigure c).

3.3. Biopore recycling

Before presenting the results of biopore recycling, note that the rest of our analysis will be focusing on the loam treatments. The analysis of the sand treatments was not carried out because the number of samples containing roots in both phase 1 and 3 was not high enough to construct a reliable statistical analysis (Fig. 2c). Also, the old root tissues posed issues when trying to properly segment the roots of phase 3 because they still exhibited a similar gray value as the alive/intact roots of phase 3. On top of that, the fragile structure of the sand created problems when trying to register the images of both phases onto each other. Indeed, finding landmarks on these images proved to be unreliable due to the movement of sand grains (Fig. 3b).

The calculated BRF values were in the range of 0–0.024 and there was no statistical difference between the high and the low bulk density treatments in loam (p-value = 0.46) (Fig. 4a). The calculated NCP values were in the range of 0–2.8 cm^{-3} and there were also no significant differences between the two bulk density treatments (p-value = 0.27) (Fig. 4b). Since no differences between the high and the low bulk density treatments were found, both datasets were pooled together for the subsequent analyses. Plotting the relationship between the BRF and the NPC showed a positive correlation between the two variables (R^2 = 0.23), as also supported by the p-value of the linear regression ($p < 0.001$) (Fig. 4c). The maximum value of BRF (i.e., 0.024, see the corresponding sample circled with a dashed line on Fig. 4) presented the most astonishing biopore recycling of our dataset, in which a root grew into a biopore for a length of 13.1 mm before leaving the field of view. Note that removing this sample from the regression shown in the subfigure c increases the R^2 to 0.35.

The total number of contact points (not normalized by the volume of the samples) observed for the whole dataset was 438. Out of those contact points, the number of occurrences of a root being deflected and colonizing a biopore upon hitting it was only 10. That is, only approximately 2% of the roots grew into a biopore when they had the opportunity to do so. Most contact points were in fact roots crossing the biopores. Visual examples of a root crossing a biopore or colonizing it are shown in Fig. 5a and b, respectively.

For those instances for which biopore recycling was observed, we found that the contact angle between the roots and the biopores was inferior to 45 degrees for nine instances out of ten. The average contact angle was 31.8 degrees (± 5.7 degrees standard error; n = 10). Interestingly, the diameter of the roots reusing the biopores was approximately equal to the diameter of the biopores for eight instances out of those ten contact points. For the two remaining instances of biopores recycling, the diameter of the roots reusing the biopores was smaller than the diameter of the biopores. After entering the biopores, the roots continued their growth for an average distance of 5.8 mm (± 1 mm standard error; n = 10) before diverting into the soil again or leaving the ingrowth cores.

Note that the angle between the roots and the biopores was not an exclusive criterion, i.e., many contact points with crossings had a contact angle inferior to 45 degrees. However, the contact angle between roots and biopores was significantly higher when roots were crossing the biopores ($p < 0.001$). For those contact points where roots were crossing the biopores, 14 out of 15 randomly chosen contact points had a contact angle superior to 45 degrees. The average contact angle was 63.9 degrees (± 6.4 degrees standard error; n = 15). For those 15 crossing points which were visually analyzed, the diameter of the roots and biopores were approximately equal for eight instances. For the seven remaining crossing points, the root diameter was bigger than the diameter of the biopores.

3.4. Model comparison

For both the phase 1 and 3, the RLD simulated with CPlantBox matched the experimentally measured RLD profile pretty well, as assessed by the small relative root mean square error (rRMSE = 21% and rRMSE = 31% for phase 1 and phase 3 respectively, see Fig. S5a). The fit of CPlantBox for the mean root diameter was also good (rRMSE = 14% and rRMSE = 26% for phase 1 and phase 3 respectively, see Fig. S5b). The fit of the generalized additive model to the experimental and modelled data provided good results, as assessed by a relatively high adjusted R^2 (R^2 = 0.917) and deviance explained (91%).

For both the experimental and modelled data, the predicted NCP for all combinations of BLD and RLD showed an increase from the left bottom corner (low BLD and RLD) to the upper right corner (high BLD and RLD) of the 2D smooth surfaces (Fig. 6a and b). This increase was stronger for the modelled dataset, which led to higher predicted NCP values for the model as compared to the experiment. For high BLD and RLD, the NCP values were approximately equal to 6 cm^{-3} for the model as opposed to 3 for the experiment. The calculation of 2D smooth surface of $NCP_{exp} - NCP_{mod}$ illustrate also this difference well (Fig. 6c). The difference between the modelled and experimental data also shows a strong diagonal gradient from bottom to top. At no point, the calculation of $NCP_{exp} - NCP_{mod}$ yielded positive values. According to the hypothesis related to our methodology, this suggests that roots never showed a preference for growing towards biopores. Keeping the methodological hypothesis in mind, roots rather exhibited indifference towards biopores (i.e., at low BLD and RLD) or avoidance of biopores (i.e., at high BLD and RLD). Yet, this avoidance is rather speculative, as no experimental

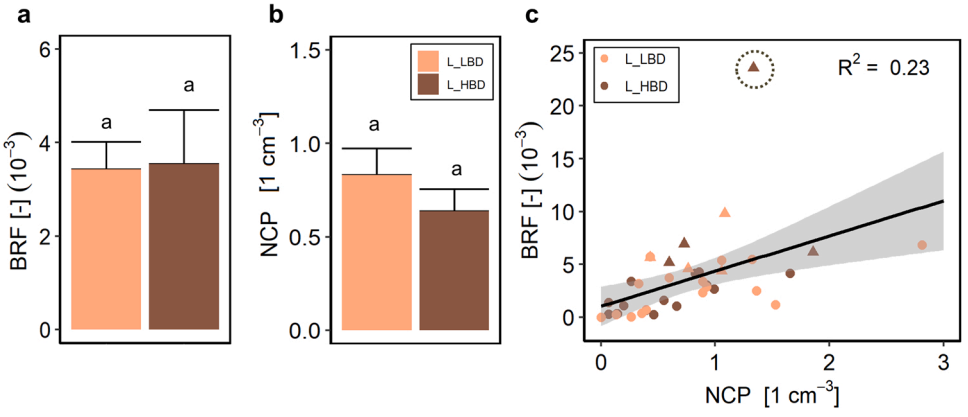

Fig. 4. The biopore recycling fraction (BRF, subfigure a) and the normalized number of contact points (NCP, subfigure b) for the high and low bulk density treatments in loam. Error bars respresent the standard error of the measurements. The letters indicate the statistical comparison of the two independent treatment according to a Wilcoxon test considering $\alpha = 0.05$. c) The relationship between the NCP and BRF calculated for both the low and high bulk density treatments in loam. The shaded gray bands represent the 95% confidence level interval for predictions from the linear model. The maximum value of BRF (see sample circled with a dashed line) presented the most astonishing biopore recycling of our dataset, in which a root grew into a biopore for a length of 13.1 mm before leaving the field of view. Note that removing this sample from the regression shown in the subFig. c increases the R^2 to 0.35. The triangles denote the samples for which at least one instance of biopore recycling was observed within the sample, whereas the dots denote the samples for which no instance of biopore recycling was observed.

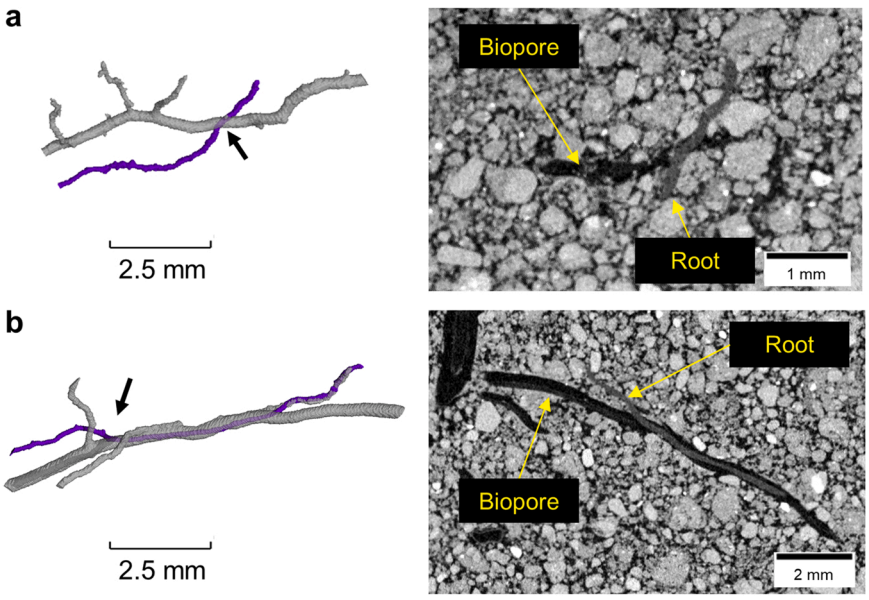

Fig. 5. Illustration of a root piercing through or reusing a biopore. a) 3D representation of a root (purple) piercing through a biopore (semi-transparent gray) and its corresponding 2D cross-sectional gray scale image at the point of piercing. b) 3D representation of a root (purple) growing into a biopore (semi-transparent gray) and its corresponding 2D cross-sectional gray scale image. The black arrow indicates the point of entry of the root into the biopore. The case of a root piercing through a biopore (subfigure a) was the most commonly observed in our dataset.

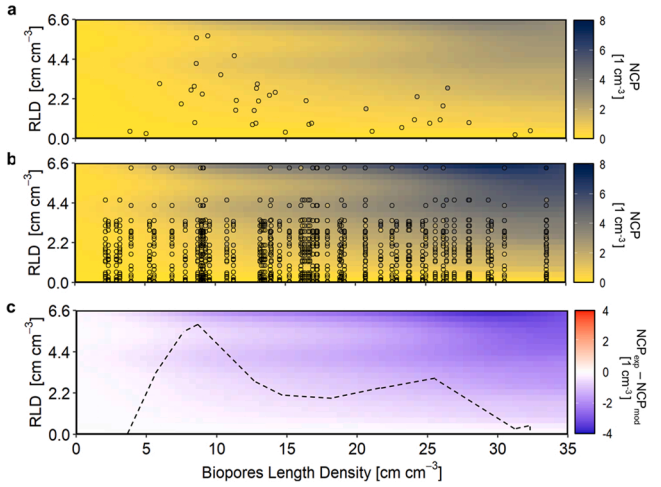

Fig. 6. Comparison between the modelled and the experimental NCP values. a) The 2D smooth surface for the experimental dataset, with the experimental data point shown on top of the surface. b) The 2D smooth surface for the modelling dataset, with the modelling data point shown on top of the surface. For both the experimental and modelling dataset, a positive gradient is observed in the upward diagonal direction, i.e., the higher the BLD and RLD, the more roots touch biopores. c) The difference of the 2D smooth surface for the modelling dataset and the experiment dataset. According to our methological hypoethesis, positive values of this difference indicate a tendency of roots to avoid biopores. The dashed line depicts the BLD and RLD range of values observed in the experimental dataset. Interpreting the values outside of this range is extrapolation.

observations were available for that BLD-RLD range.

4. Discussion

4.1. Biopore recycling

The degree of biopore recycling observed in our experiment was very low, with a mean value of approximately 0.0036 cm root cm^{-1} biopore. Despite the different methods of investigation and the use of different units to characterize biopore reuse, higher values of two orders of magnitude of biopore recycling were previously reported in the literature (Athmann et al., 2013; Han et al., 2017; Nakamoto, 1997, 2000). A X-ray CT study comparable to ours, yet with artificial macropores, reported values of 0.11 – 0.14 contacts cm^{-1} biopore for different plant species in compacted soil, with varying fractions of contacts leading to colonization (Colombi et al., 2017). The average colonization length was not reported but would in all cases lead to BRF values that are at least two orders of magnitude larger. Likewise, approximately 0.4 contacts cm^{-1} biopore were reported for wheat roots irrespective of bulk density (1.2 g cm^{-3} vs. 1.6 g cm^{-3}), yet with a clear shift towards colonization for the compacted soil (Atkinson et al., 2020). Moreover, the fraction of colonization events per contact point was much lower in our study (2%) than in comparable pot experiments with artificial macropores (13 – 69%) (Atkinson et al., 2020; Colombi et al., 2017; Pfeifer et al., 2014) This difference between the present and previous studies can be explained by several reasons, namely the mechanical impedance, the oxygen and nutrient status, the origin of the biopores and the inclusion of biopores having a small diameter in our analysis.

The first reason which would explain the small degree of biopore recycling in our experiment is mechanical impedance. Indeed, at the water content investigated in the present experiment, penetration resistance was approximately 0.15 MPa (Fig. S1. U. Rosskopf, S. Peth, D. Uteau, University Hannover, personal communication) for the low bulk density treatment of loam (1.26 g cm^{-3}). The high bulk density treatment (1.36 g cm^{-3}) was at the lower end of values (1.3 – 1.5 g cm^{-3}) observed in a field trial with the same loam material for which penetration resistance was below 1.5 MPa. These values are well below the critical value for root elongation of 2 MPa suggested by Bengough et al. Considering this, there might have been no need for the roots to grow into the available biopores as they could easily explore the available soil volume without restriction to root elongation. An increase in bulk density from 1.26 g cm^{-3} to 1.36 g cm^{-3} did not result in a significantly higher degree of biopore recycling. This is contrary to our original assumption and conflicting with the results of Hirth et al. (2005) who showed that an increasing bulk density increased the percentage of root length found in biopores which were inclined with an angle of 40 degrees from the horizontal plane. More extreme compaction of the substrate could have led to more pronounced effects of soil bulk density and to some higher degree of biopore recycling, but might also have drastically reduced root growth in the repacked soil columns investigated.

A second reason potentially explaining the low degree of biopore recycling is the nutrient and oxygen availability. In this column experiment, the substrate were previously fertilized in the same fashion as in

Lippold et al. (2021) in order to ensure an adequate plant and root growth. Also, the volumetric water content was kept at an average value of 22% (Fig. S4). This value corresponds to an air-filled fraction of the total pore space of approximately 56%. In the literature, some authors suggest that the reuse of biopores is triggered by the nutrient and oxygen shortage in the subsoil and the enrichment of the biopores in nutrients, soil organic carbon, microbial biomass and oxygen beneficial to plant and root growth (Athmann et al., 2014; Colombi et al., 2017; Edwards and Lofty, 1980; Stewart et al., 1999). The reason as to why root growth in biopores was so low in our experiment might be related to the fact that nutrients and oxygen were available in sufficient quantity due to the fertilization and the well-aerated conditions in the soil columns of our experiment.

The nature of the biopores can also provide an explanation for the low degree of biopore recycling in our experiment. In the literature, many studies reported root growth into biopores in field conditions (Athmann et al., 2013; Han et al., 2017, 2015) or intact soil cores (Zhou et al., 2021), where the genesis, the history and the usage of the biopores is rarely documented because of the difficulties associated with the determination of these characteristics. Depending on their age and history of utilisation (crop rotation, earthworm passage, preferential flow), individual biopores can differ widely in their physical conditions (Pagenkemper et al., 2015) and nutrient status (Kautz et al., 2014). Some studies have also investigated biopore recycling under somewhat unrealistic condtions, i.e., by artificially creating vertical holes by pushing a rod or a wire into the soil (Atkinson et al., 2020; Colombi et al., 2017; Dresemann et al., 2018; Hirth et al., 2005; Nakamoto, 1997; Pfeifer et al., 2014; Stirzaker et al., 1996). Under these conditions, the trapping of roots in the biopores is more likely to occur considering the inherent gravitopism that roots exhibit. Artificial pores are also likely to have a greater compaction and a smoother surface at the pore wall, both of which are known to exacerbate root trapping in biopores (Hirth et al., 2005; Stirzaker et al., 1996). Obviously, the comparison of our results with those studies is delicate. Indeed, our study focused exclusively on biopores which extended more laterally than vertically, considering that primary roots were only rarely captured during the extraction of the ingrowth cores. Moreover, the biopores in our experiment were young, induced exclusively by *Zea mays* L. plants and potentially reused exclusively by the roots of *Zea mays* L. plants. This may also have contributed to the low degree of biopore recycling. Indeed, Rasse and Smucker (1998) highlighted the importance of crop succession by showing that biopore recycling of maize after maize was lower than if maize was succeeding alfalfa.

Finally, another potential explanation for the differences between the biopore recycling observed in our study and the values previously reported in the literature is the inclusion of biopores of diameter down to 60 μm in our analysis. Indeed, previous studies on biopore recycling only focused on a fairly large biopore diameter class (e.g., $\geq$ 400 μm in Nakamoto, 2000, $\geq$ 3.8 mm in Athmann et al., 2013, $\approx$ 3.2 mm in Stirzaker et al., 1996 or only biopores visible to the naked eye for Nakamoto, 1997). Excluding the small biopore diameter class from their analysis inherently omits a huge proportion of the existing biopores in soil. Strictly mathematically speaking, calculating "the proportion of roots in biopores" (Nakamoto, 1997, 2000) or "the percentage of biopores with roots" (Athmann et al., 2013) while omitting a big fraction of biopores results in greatly decreasing the denominator of the fraction, thereby greatly increasing the estimation of biopore recycling. In our study with biopores induced by *Zea mays* L. and a high detection of small roots/biopores (i.e., an image resolution of 19 μm), approximately 97% of the roots fell into the diameter class $\leq$ 400 μm (Table S1). In contrast, artificial macropores typically have a diameter of $>$ 800 μm for technical reasons (Atkinson et al., 2020; Colombi et al., 2017; Pfeifer et al., 2014) therefore targeting a completely different type of root-biopore interaction. By capturing these small biopores, the resulting biopore recycling fraction calculated in our study is inevitably much lower than previously reported in the literature.

Comparing the experimental data and the modelled data allowed drawing conclusions regarding the behavior of roots towards biopores. By doing so, we found that roots tended to be indifferent to biopores. The reasons as to why roots were indifferent to biopores are currently still unknown. In a very speculative manner, we suggest that this behavior could be explained by the fact that the wall of the biopores in our experiment might have already been depleted in nutrients, as observed by Hendriks et al. (1981), and/or colonized by some pathogens as suggested by Rasse and Smucker (1998). Both of these explanations would support the argument that root growth was favored in regions of the soil column where the nutrient content was higher and the pathogenic pressure lower. Note that our study supports the findings of Dexter (1986) who also found no evidence for the roots sensing and growing preferentially towards the holes in the well-aerated system used in his experiments.

4.2. *Influence of soil texture*

The effect of soil texture on biopore recycling could not be directly investigated as originally intended and stated in the first hypothesis of our work. Due to the low number of samples containing roots in phase 1 and phase 3 and to the technical difficulties related to the processing of those images (segmentation and registration), the analysis of BRF and NPC was not carried out for the sand treatment. Also in loam, we did not derive quantitative decomposition rates due to the small number of time points and scanned samples. A more rigorous image-based analysis can lead to more insights in the future. However, some qualitative information regarding the nature and stability of biopores in a loam and a sand soil could be gained. In loam, roots completely degraded in a short period of time (less than 78 days of incubation at 25 °C under moist conditions) and the biopores that the roots left behind were structurally stable over time. In sand, old root tissues were still found in biopores 216 days after their creation under the same incubation conditions. On some occasions, the biopores in sand were also found to be partially or completely refilled due to the subsidence and lateral displacement of sand grains in the vicinity of the biopores. Considering this, biopore recycling in sandy soils is much less likely to occur as compared to in loamy soils. Note that the lower stability of biopores in sandy in comparison to loamy soils has already been suggested by Schneider and Don (2019).

The influence of soil texture on the decomposition of root tissues has already been observed by other studies (Gijsman et al., 1997; Scott et al., 1996). This difference has been attributed to differences in water and gas regime (Gijsman et al., 1997; Haling et al., 2013), both of which are known to alter the microbial activity in soil (Angst et al., 2021; Borowik and Wyszkowska, 2016; Schjønning et al., 2003). Microbial activity was supposedly much lower in the bulk soil of sand due to the high proportion of quartz added to the mixture which might have also resulted in lower microbial activity in the rhizosphere and thus lower decomposition rates. Note that, in our study, the fact that root residues were still present in the biopores in sand might also be due to the fact that roots in sand grew bigger in diameter (Fig. S6). Possibly, the decomposition rate of the roots was the same for the loam and the sand, but the decomposition of the roots in sand was not yet complete since more matter had to be decomposed in the same amount of time. Note that the increase in diameter of roots was already reported by Lippold et al. (2021) for the same substrates, but no explanation for this increase has been found yet.

Soil texture also has an influence on the nature of the biopores themselves, more precisely on the degree of compaction of their walls. Using the same substrate and bulk density treatments as in the present study, Phalempin et al. (2021b) demonstrated that soil texture was a predominant factor which governed the bulk density gradients around roots, and hence, on the level of compaction of the walls of the biopores. For the loam and sand investigated in this experiment, differences in the compaction of the soil in the vicinity of roots were also observed (Fig. 3). Indeed, the rhizosphere soil was more compacted in loam as compared

to in sand (see also Fig. 3 in Phalempin et al., 2021b). These differences may lead to different tendencies of the roots to be "trapped" in biopores, as already suggested by Stirzaker et al. (1996), Stewart et al. (1999) and Nakamoto (2000). In our experiment, we did not observe roots being trapped as most roots were crossing the biopores and those which colonized biopores escaped them only after a short distance (on average 5.8 mm).

4.3. Limitations and future work

In this paper, we presented a novel methodology for the study of biopore recycling with the help of X-ray CT and *in silico*. Our modelling approach integrated 3D root architecture information and therefore combined much more information in comparison to previous simulation studies, which focused on soil 2D thin sections (Stewart et al., 1999) or on the simple application of probabilistic laws (Nakamoto, 1997; Stirzaker et al., 1996). With this methodology, we further introduced a new metric (i.e., the normalized number of contact points) to characterize the behavior of roots towards biopores. The new approach also allowed determining the effect of the biopore length density and the root length density on the normalized number of contact points. To the best of our knowledge, such a modelling effort has not been undertaken before.

One limitation of our approach is related to the range of biopore length density and root length density covered by our analysis. By constraining root growth in a pot, the biopore length density that was created during phase 1 was much higher than the biopore length density which can be expected in field conditions. Lucas et al. (2019) showed that root length density was as low as 1.83 cm cm^{-3} after one year of reclamation of a mining area and that biopore length density reached a plateau of 18.79 cm cm^{-3} for the interval 0 – 20 cm depth after six years of reclamation. In our study, the biopore length density observed was approximately two times higher than the expected biopore length density after reaching equilibrium, which might not be realistic compared to natural conditions. For the root length density observed during phase 3, however, the values observed in our study are well in line with the values which can be expected in the field after one season of growth (Lucas et al., 2019; Phalempin et al., 2021b).

In our study, we investigated biopore recycling for a crop succession of maize after maize. Future work should orient towards implementing the presented methodology to multi-species succession to find out whether others species behave in a similar manner as compared to the maize-maize succession investigated in this experiment. Finally, the natural continuation of this work is to include the presence of biopores in the initial conditions of the root growth modelling of phase 3. This would make it possible to explicitly model root growth in biopores as in Landl et al. (2019).

5. Conclusion

In this study, we developed a novel methodology to characterize the degree of biopore recycling occurring in repacked soil columns under controlled conditions. The novel methodology is based on the repeated scanning of soil samples and co-registration of the acquired images after the creation of biopores and their potential reuse. With this methodology, we showed that the degree of biopore recycling in repacked loam was low, i.e., on average 0.0036 centimeters of roots were found in 1 centimeter of biopore, which was two orders of magnitude lower than the values previously reported in the literature. We attributed this difference to the low mechanical impedance, the good nutrient and aeration status in the repacked soil columns and to the inclusion of biopores of small diameter in our analysis. In our experiment, roots were most prominently crossing the biopores instead of colonizing them. Root growth inside biopores was only anecdotally observed and amounted to 2% of all root-biopore contacts. Visual analysis of the images showed that the propensity of roots to grow into biopores was higher when the angle at which roots and biopores touched was inferior to 45 degrees and when the root diameter was approximately equal to or inferior to the biopore diameter. The effect of bulk density on the biopore recycling fraction and on the normalized number of contact points was not statistically significant in the investigated range.

The visual analysis of intermittent X-ray CT scans provided insights into the degradation of roots and the behavior of biopores in two soils with contrasted textures. In loam, the roots were completely degraded in a short period of time (less than 78 days) and the biopores that the roots left behind were structurally stable over time. In sand, old root tissues were still found in biopores 216 days after their creation. When full root decomposition was observed in sand, many biopores had collapsed due to the weak cohesive forces between the coarse sand grains. Both effects together render biopore recycling in sand unlikely to occur.

In addition to the analysis of the experimental data, we introduced a new methodology which made it possible to characterize the behavior of roots towards biopores. This methodology relies on the use of the stochastic root growth model CPlantBox and the comparison with the experimental data. With this new approach, we showed that roots were indifferent to natural biopores, in well aerated, fertilized and repacked soil columns.

Author contributions

MP, DV and SS designed the study. MP established the experimental set-up, scanned the samples with X-ray CT, carried out the image processing steps and analyzed the results. ML carried out the modelling approach. MP wrote the original draft and produced the figures. All authors discussed data analysis approaches, read and edited the manuscript.

Declaration of Competing Interest

The authors declare that they have no known competing financial interests or personal relationships that could have appeared to influence the work reported in this paper.

Data Availability

The data used in this study is available from the corresponding author upon reasonable request. The generated data for the modelling approach with CPlantBox is available in the GitHub repository under the following link: https://github.com/Plant-Root-Soil-Interactions-Modelling/CPlantBox/tree/pub_phalempin_2021/tutorial/examples/Phalempin_2021.

Acknowledgments

This project was carried out in the framework of the priority programme 2089 "Rhizosphere spatiotemporal organisation - a key to rhizosphere functions" funded by DFG, German Research Foundation (project number 403801423 and 403641034). Seeds of the maize wild-type were provided by Caroline Marcon and Frank Hochholdinger (University of Bonn).

Appendix A. Supporting information

Supplementary data associated with this article can be found in the online version at doi:10.1016/j.still.2022.105398.

References

Angst, G., Pokorný, J., Mueller, C.W., Prater, I., Preusser, S., Kandeler, E., Meador, T., Straková, P., Hájek, T., van Buiten, G., Angst, Š., 2021. Soil texture affects the coupling of litter decomposition and soil organic matter formation. Soil Biol. Biochem. 159, 108302 https://doi.org/10.1016/j.soilbio.2021.108302.

Athmann, M., Kautz, T., Huang, N., Köpke, U., 2014. Biopore characterization with in situ endoscopy: influence of earthworms on carbon and nitrogen contents. Build. Org. Bridges 2, 415–418. https://doi.org/10.3220/REP_20_1_2014.
Athmann, M., Kautz, T., Pude, R., Köpke, U., 2013. Root growth in biopores—evaluation with in situ endoscopy. Plant Soil 371 (1), 179–190. https://doi.org/10.1007/s11104-013-1673-5.
Atkinson, J.A., Hawkesford, M.J., Whalley, W.R., Zhou, H., Mooney, S.J., 2020. Soil strength influences wheat root interactions with soil macropores. Plant Cell Environ. 43 (1), 235–245. https://doi.org/10.1111/pce.13659.
Banfield, C.C., Zarebanadkouki, M., Kopka, B., Kuzyakov, Y., 2017. Labelling plants in the Chernobyl way: a new 137Cs and 14C foliar application approach to investigate rhizodeposition and biopore reuse. Plant Soil 417 (1), 301–315. https://doi.org/10.1007/s11104-017-3260-7.
Barej, J.A.M., Pätzold, S., Perkons, U., Amelung, W., 2014. Phosphorus fractions in bulk subsoil and its biopore systems. Eur. J. Soil Sci. 65 (4), 553–561. https://doi.org/10.1111/ejss.12124.
Bauke, S.L., Landl, M., Koch, M., Hofmann, D., Nagel, K.A., Siebers, N., Schnepf, A., Amelung, W., 2017. Macropore effects on phosphorus acquisition by wheat roots – a rhizotron study. Plant Soil 416 (1), 67–82. https://doi.org/10.1007/s11104-017-3194-0.
Bengough, A.G., Mullins, C.E., 1990. Mechanical impedance to root growth: a review of experimental techniques and root growth responses. J. Soil Sci. 41 (3), 341–358. https://doi.org/10.1111/j.1365-2389.1990.tb00070.x.
Borowik, A., Wyszkowska, J., 2016. Soil moisture as a factor affecting the microbiological and biochemical activity of soil. Plant Soil Environ. 62 (6), 250–255. https://doi.org/10.17221/158/2016-PSE.
Cheik, S., Jouquet, P., Maeght, J.-L., Capowiez, Y., Tran, T.M., Bottinelli, N., 2021. X-ray tomography analysis of soil biopores structure under wetting and drying cycles. Eur. J. Soil Sci. 1–5. https://doi.org/10.1111/ejss.13119.
Colombi, T., Braun, S., Keller, T., Walter, A., 2017. Artificial macropores attract crop roots and enhance plant productivity on compacted soils. Sci. Total Environ. 574, 1283–1293. https://doi.org/10.1016/j.scitotenv.2016.07.194.
Crawford, R.M.M., 1992. Oxygen availability as an ecological limit to plant distribution. In: Begon, M., Fitter, A.H. (Eds.), Advances in Ecological Research, Vol. 23. Academic Press, pp. 93–185. https://doi.org/10.1016/S0065-2504(08)60147-6.
Dexter, A.R., 1986. Model experiments on the behaviour of roots at the interface between a tilled seed-bed and a compacted sub-soil. Plant Soil 95 (1), 149–161. https://doi.org/10.1007/BF02378860.
Dohnal, M., Dušek, J., Vogel, T., Císlerová, M., Lichner, Ľ., Štekauerová, V., 2009. Ponded infiltration into soil with biopores — field experiment and modeling. Biologia 64 (3), 580–584. https://doi.org/10.2478/s11756-009-0078-7.
Doube, M., Kłosowski, M.M., Arganda-Carreras, I., Cordelières, F.P., Dougherty, R.P., Jackson, J.S., Schmid, B., Hutchinson, J.R., Shefelbine, S.J., 2010. BoneJ: free and extensible bone image analysis in ImageJ. Bone 47 (6), 1076–1079. https://doi.org/10.1016/j.bone.2010.08.023.
Dresemann, T., Athmann, M., Heringer, L., Kautz, T., 2018. Effects of continuous vertical soil pores on root and shoot growth of winter wheat: a microcosm study. Agric. Sci. 9 (6), 750–764. https://doi.org/10.4236/as.2018.96053.
Edwards, C.A., Lofty, J.R., 1980. Effects of earthworm inoculation upon the root growth of direct drilled cereals. J. Appl. Ecol. 17 (3), 533–543. https://doi.org/10.2307/2402635.
Ehlers, W., 1975. Observations on earthworn channels and infiltration on tilled and untilled loess soil. Soil Sci. 119 (3) https://doi.org/10.1097/00010694-197503000-00010.
Filleur, S., Walch-Liu, P., Gan, Y., Forde, B.G., 2005. Nitrate and glutamate sensing by plant roots. Biochem. Soc. Trans. 33 (1), 283–286. https://doi.org/10.1042/BST0330283.
Fletcher, R., 2013. Practical Methods of Optimization. John Wiley & Sons.
Fox, J., Weisberg, S., Adler, D., Bates, D., Baud-Bovy, G., Ellison, S., Firth, D., Friendly, M., Gorjanc, G., & Graves, S. (2012). Package 'car'. *Vienna: R Foundation for Statistical Computing*, 16.
Gijsman, A.J., Alarcón, H.F., Thomas, R.J., 1997. Root decomposition in tropical grasses and legumes, as affected by soil texture and season. Soil Biol. Biochem. 29 (9), 1443–1450. https://doi.org/10.1016/S0038-0717(97)00039-4.
Gliński, J., Lipiec, J., 2018. Soil Physical Conditions and Plant Roots. CRC Press. https://doi.org/10.1201/9781351076708.
Hagedorn, F., Bundt, M., 2002. The age of preferential flow paths. Geoderma 108 (1), 119–132. https://doi.org/10.1016/S0016-7061(02)00129-5.
Haling, R.E., Tighe, M.K., Flavel, R.J., Young, I.M., 2013. Application of X-ray computed tomography to quantify fresh root decomposition in situ. Plant Soil 372 (1), 619–627. https://doi.org/10.1007/s11104-013-1777-y.
Han, E., Kautz, T., Huang, N., Köpke, U., 2017. Dynamics of plant nutrient uptake as affected by biopore-associated root growth in arable subsoil. Plant Soil 415 (1), 145–160. https://doi.org/10.1007/s11104-016-3150-4.
Han, E., Kautz, T., Perkons, U., Uteau, D., Peth, S., Huang, N., Horn, R., Köpke, U., 2015. Root growth dynamics inside and outside of soil biopores as affected by crop sequence determined with the profile wall method. Biol. Fertil. Soils 51 (7), 847–856. https://doi.org/10.1007/s00374-015-1032-1.
Hendriks, L., Claassen, N., Jungk, A., 1981. Phosphatverarmung des wurzelnahen Bodens und Phosphataufnahme von Mais und Raps. Z. Fur Pflanzenernahr. Und Bodenkd. 144 (5), 486–499.
Hensen, V., 1892. Die Wurzeln in den tieferen Bodenschichten. Jahrb. der Dtsch. Landwirtsch. -Ges. 7, 84–96.
Hernanz, J.L., Peixoto, H., Cerisola, C., Sánchez-Girón, V., 2000. An empirical model to predict soil bulk density profiles in field conditions using penetration resistance, moisture content and soil depth. J. Terra 37 (4), 167–184. https://doi.org/10.1016/S0022-4898(99)00020-8.
Hirth, J.R., McKenzie, B.M., Tisdall, J.M., 2005. Ability of seedling roots of Lolium perenne L. to penetrate soil from artificial biopores is modified by soil bulk density, biopore angle and biopore relief. Plant Soil 272 (1), 327–336. https://doi.org/10.1007/s11104-004-5764-1.
Hothorn, T., Bretz, F., Westfall, P., 2008. Simultaneous inference in general parametric models. Biom. J. 50 (3), 346–363. https://doi.org/10.1002/bimj.200810425.
Jones, D.L., Nguyen, C., Finlay, R.D., 2009. Carbon flow in the rhizosphere: carbon trading at the soil–root interface. Plant Soil 321 (1), 5–33. https://doi.org/10.1007/s11104-009-9925-0.
Kautz, T., 2015. Research on subsoil biopores and their functions in organically managed soils: a review. Renew. Agric. Food Syst. 30 (4), 318–327. https://doi.org/10.1017/S1742170513000549.
Kautz, T., Athmann, M., Köpke, U., 2014. Growth of barley (Hordeum vulgare L.) roots in biopores with differing carbon and nitrogen contents. Build. Org. Bridges 2, 391–394. https://doi.org/10.3220/REP_20_1_2014.
Kautz, T., Köpke, U., 2010. In situ endoscopy: New insights to root growth in biopores. Plant Biosyst. - Int. J. Deal. Asp. Plant Biol. 144 (2), 440–442. https://doi.org/10.1080/11263501003726185.
Klein, S., Staring, M., Murphy, K., Viergever, M.A., Pluim, J.P.W., 2010. elastix: a toolbox for intensity-based medical image registration. IEEE Trans. Med. Imaging 29 (1), 196–205. https://doi.org/10.1109/TMI.2009.2035616.
Landl, M., Haupenthal, A., Leitner, D., Kroener, E., Vetterlein, D., Bol, R., Vereecken, H., Vanderborght, J., Schnepf, A., 2021. Simulating rhizodeposition patterns around growing and exuding root systems. Silico Plants. https://doi.org/10.1093/insilicoplants/diab028.
Landl, M., Schnepf, A., Uteau, D., Peth, S., Athmann, M., Kautz, T., Perkons, U., Vereecken, H., Vanderborght, J., 2019. Modeling the impact of biopores on root growth and root water uptake. Vadose Zone J. 18 (1), 180196 https://doi.org/10.2136/vzj2018.11.0196.
Legland, D., Arganda-Carreras, I., Andrey, P., 2016. MorphoLibJ: integrated library and plugins for mathematical morphology with ImageJ. Bioinformatics 32 (22), 3532–3534. https://doi.org/10.1093/bioinformatics/btw413.
Lippold, E., Phalempin, M., Schlüter, S., Vetterlein, D., 2021. Does the lack of root hairs alter root system architecture of Zea mays? Plant Soil. https://doi.org/10.1007/s11104-021-05084-8.
Lucas, M., Schlüter, S., Vogel, H.-J., Vetterlein, D., 2019. Soil structure formation along an agricultural chronosequence. Geoderma 350, 61–72. https://doi.org/10.1016/j.geoderma.2019.04.041.
Lucas, M., Vetterlein, D., Vogel, H.-J., Schlüter, S., 2021. Revealing pore connectivity across scales and resolutions with X-ray CT. Eur. J. Soil Sci. 72 (2), 546–560. https://doi.org/10.1111/ejss.12961.
McCormick, M.M., Liu, X., Ibanez, L., Jomier, J., Marion, C., 2014. ITK: enabling reproducible research and open science. Front. Neuroinform. 8, 13. https://doi.org/10.3389/fninf.2014.00013.
Nakamoto, T., 1997. The distribution of maize roots as influenced by artificial vertical macropores. Jpn. J. Crop Sci. 66 (2), 331–332. https://doi.org/10.1626/jcs.66.331.
Nakamoto, T., 2000. The distribution of wheat and maize roots as influenced by biopores in a subsoil of the kanto loam type. Plant Prod. Sci. 3 (2), 140–144. https://doi.org/10.1626/pps.3.140.
Ollion, J., Cochennec, J., Loll, F., Escudé, C., Boudier, T., 2013. TANGO: a generic tool for high-throughput 3D image analysis for studying nuclear organization. Bioinformatics 29 (14), 1840–1841. https://doi.org/10.1093/bioinformatics/btt276.
Pagenkemper, S.K., Athmann, M., Uteau, D., Kautz, T., Peth, S., Horn, R., 2015. The effect of earthworm activity on soil bioporosity – investigated with X-ray computed tomography and endoscopy. Soil Tillage Res. 146, 79–88. https://doi.org/10.1016/j.still.2014.05.007.
Pankhurst, C.E., Pierret, A., Hawke, B.G., Kirby, J.M., 2002. Microbiological and chemical properties of soil associated with macropores at different depths in a red-duplex soil in NSW Australia. Plant Soil 238 (1), 11–20. https://doi.org/10.1023/A:1014289632453.
Passioura, J.B., 2002. Soil conditions and plant growth. Plant Cell Environ. 25 (2), 311–318. https://doi.org/10.1046/j.0016-8025.2001.00802.x.
Pfeifer, J., Kirchgessner, N., Walter, A., 2014. Artificial pores attract barley roots and can reduce artifacts of pot experiments. J. Plant Nutr. Soil Sci. 177 (6), 903–913. https://doi.org/10.1002/jpln.201400142.
Phalempin, M., Lippold, E., Vetterlein, D., Schlüter, S., 2021a. An improved method for the segmentation of roots from X-ray computed tomography 3D images: rootine v. 2. Plant Methods 17 (1), 1–19. https://doi.org/10.1186/s13007-021-00735-4.
Phalempin, M., Lippold, E., Vetterlein, D., Schlüter, S., 2021b. Soil texture and structure heterogeneity predominantly governs bulk density gradients around roots. Vadose Zone J., e20147 https://doi.org/10.1002/vzj2.20147.
Rasse, D.P., Smucker, A.J.M., 1998. Root recolonization of previous root channels in corn and alfalfa rotations. Plant Soil 204 (2), 203–212. https://doi.org/10.1023/A:1004343122448.
Rosskopf, U., Uteau, D., Peth, S., 2022. Development of mechanical soil stability in an initial homogeneous loam and sand under in-situ field conditions, 2022/02/10 Plant Soil. https://doi.org/10.21203/rs.3.rs-1181463/v1.
Schindelin, J., Arganda-Carreras, I., Frise, E., Kaynig, V., Longair, M., Pietzsch, T., Preibisch, S., Rueden, C., Saalfeld, S., Schmid, B., 2012. Fiji: an open-source platform for biological-image analysis. Nat. Methods 9 (7), 676–682. https://doi.org/10.1038/nmeth.2019.

Schjønning, P., Thomsen, I.K., Moldrup, P., Christensen, B.T., 2003. Linking soil microbial activity to water- and air-phase contents and diffusivities. Soil Sci. Soc. Am. J. 67 (1), 156–165. https://doi.org/10.2136/sssaj2003.1560.

Schneider, F., Don, A., 2019. Root-restricting layers in German agricultural soils. Part II: adaptation and melioration strategies. Plant Soil 442 (1), 419–432. https://doi.org/10.1007/s11104-019-04186-8.

Schnepf, A., Leitner, D., Landl, M., Lobet, G., Mai, T.H., Morandage, S., Sheng, C., Zörner, M., Vanderborght, J., Vereecken, H., 2018. CRootBox: a structural–functional modelling framework for root systems. Ann. Bot. 121 (5), 1033–1053. https://doi.org/10.1093/aob/mcx221.

Scott, N.A., Cole, C.V., Elliott, E.T., Huffman, S.A., 1996. Soil textural control on decomposition and soil organic matter dynamics. Soil Sci. Soc. Am. J. 60 (4), 1102–1109.

Shamonin, D., Bron, E., Lelieveldt, B., Smits, M., Klein, S., Staring, M., 2014. Fast parallel image registration on CPU and GPU for diagnostic classification of Alzheimer's disease. Front. Neuroinform. 7 (50) https://doi.org/10.3389/fninf.2013.00050.

Smettem, K.R.J., Collis-George, N., 1985. Statistical characterization of soil biopores using a soil peel method. Geoderma 36 (1), 27–36. https://doi.org/10.1016/0016-7061(85)90061-8.

Stewart, J.B., Moran, C.J., Wood, J.T., 1999. Macropore sheath: quantification of plant root and soil macropore association. Plant Soil 211 (1), 59–67. https://doi.org/10.1023/A:1004405422847.

Stirzaker, R., Passioura, J., Wilms, Y., 1996. Soil structure and plant growth: impact of bulk density and biopores. Plant Soil 185 (1), 151–162. https://doi.org/10.1007/BF02257571.

Tristán-Vega, A., García-Pérez, V., Aja-Fernández, S., Westin, C.-F., 2012. Efficient and robust nonlocal means denoising of MR data based on salient features matching. Comput. Methods Prog. Biomed. 105 (2), 131–144. https://doi.org/10.1016/j.cmpb.2011.07.014.

Vetterlein, D., Lippold, E., Schreiter, S., Phalempin, M., Fahrenkampf, T., Hochholdinger, F., Marcon, C., Tarkka, M., Oburger, E., Ahmed, M., Javaux, M., Schlüter, S., 2021. Experimental platforms for the investigation of spatiotemporal patterns in the rhizosphere—laboratory and field scale. J. Plant Nutr. Soil Sci. 184 (1), 35–50. https://doi.org/10.1002/jpln.202000079.

Vinther, F.P., Eiland, F., Lind, A.M., Elsgaard, L., 1999. Microbial biomass and numbers of denitrifiers related to macropore channels in agricultural and forest soils. Soil Biol. Biochem. 31 (4), 603–611. https://doi.org/10.1016/S0038-0717(98)00165-5.

Wahlström, E.M., Kristensen, H.L., Thomsen, I.K., Labouriau, R., Pulido-Moncada, M., Nielsen, J.A., Munkholm, L.J., 2021. Subsoil compaction effect on spatio-temporal root growth, reuse of biopores and crop yield of spring barley. Eur. J. Agron. 123, 126225 https://doi.org/10.1016/j.eja.2020.126225.

White, R.G., Kirkegaard, J.A., 2010. The distribution and abundance of wheat roots in a dense, structured subsoil–implications for water uptake. Plant Cell Environ. 33 (2), 133–148.

Wickham, H. (2020). Package 'plyr'. *A Grammar of Data Manipulation. R package version*, *8*.

Wickham, H., Averick, M., Bryan, J., Chang, W., McGowan, L.D.A., François, R., Grolemund, G., Hayes, A., Henry, L., Hester, J., 2019. Welcome to the Tidyverse. J. Open Source Softw. 4 (43), 1686.

Wickham, H., Chang, W., 2016. Package 'ggplot2'. *Create Elegant Data Visualisations Using the Grammar of Graphics* Version, 2, 1, pp. 1–189.

Wood, S.N., 2011. Fast stable restricted maximum likelihood and marginal likelihood estimation of semiparametric generalized linear models. J. R. Stat. Soc.: Ser. B Stat. Methodol. 73 (1), 3–36. https://doi.org/10.1111/j.1467-9868.2010.00749.x.

Wood, S.N., 2017. Generalized additive models: an introduction with R. CRC Press,.

Yunusa, I.A.M., Newton, P.J., 2003. Plants for amelioration of subsoil constraints and hydrological control: the primer-plant concept. Plant Soil 257 (2), 261–281. https://doi.org/10.1023/A:1027381329549.

Zhang, Z., Liu, K., Zhou, H., Lin, H., Li, D., Peng, X., 2018. Three dimensional characteristics of biopores and non-biopores in the subsoil respond differently to land use and fertilization. Plant Soil 428 (1), 453–467. https://doi.org/10.1007/s11104-018-3689-3.

Zhou, H., Whalley, W.R., Hawkesford, M.J., Ashton, R.W., Atkinson, B., Atkinson, J.A., Sturrock, C.J., Bennett, M.J., Mooney, S.J., 2021. The interaction between wheat roots and soil pores in structured field soil. J. Exp. Bot. 72 (2), 747–756. https://doi.org/10.1093/jxb/eraa475.